

Die explizite Schreibweise für die Faltung von drei Funktionen lautet folgendermaßen:

$$\begin{aligned} f * g * h &= f * (g * h) = \int_0^{\xi} f(\xi - x) g * h(x) dx \\ &= \int_0^{\xi} \int_y^{\xi} f(\xi - x) g(x - y) h(y) dx dy \quad (\text{A.2}) \\ &= \int_0^{\xi} dy \int_y^{\xi} f(\xi - x) g(x - y) h(y) dx. \end{aligned}$$

Durch die Substitution $x - y = \eta$ im inneren Integral in (A.2), untere Zeile, läßt sich dieser Ausdruck in

$$\begin{aligned} f * (g * h) &= \int_0^{\xi} h(y) dy \int_0^x f(\xi - y - \eta) g(\eta) d\eta \\ &= \int_0^{\xi} h(y) f * g(\xi - y) dy = h * (f * g) \quad (\text{A.3}) \\ &= (f * g) * h \end{aligned}$$

überführen (assoziatives Gesetz der Faltung).

Diese Arbeit wurde aus Mitteln des Bundesministeriums der Verteidigung ermöglicht.

¹ D. GABOR u. G. W. STROKE, *Endeavour* **23**, 40 [1969].

² S. LOWENTHAL u. H. ARSENAULT, *J. Opt. Soc. Amer.* **60**, 1478 [1970].

³ E. N. LEITH u. J. UPATNIEKS, *J. Opt. Soc. Amer.* **60**, 1478 [1970].

⁴ F. LANZL, H. J. MAGER u. W. WAIDELICH, *Z. Angew. Physik* **24**, 156 [1968].

⁵ P. BARLAI, *Z. Naturforsch.* **26 a**, 1441 [1971].

⁶ Inkohärentes Licht wird hier immer in dem Sinne quasihomogen-inkohärentes Licht verstanden.

⁷ J. W. GOODMAN, *Introduction to Fourier Optics*, McGraw-Hill, New York 1968.

⁸ W. MARTIENSEN u. E. SPILLER, *Phys. Letters* **24 A**, 126 [1967].

⁹ Es gibt mehrere Arten von Inkohärenz, die in ihrer Wirkung auf Granulationsausmittlung gleichwertig sind. Hier wird von der Tatsache Gebrauch gemacht, daß die den Bildpunkten entsprechenden Transversalmoden einer inkohärenten Lichtquelle zueinander inkohärent sind zum Unterschied von der in ⁵ angegebenen Methode der Granulationsausmittlung, wo ein punktförmiges Rekonstruktionszentrum, also nur ein Transversalmodus, verwendet wird. Dort entsteht die erforderliche Inkohärenz durch simultane, inkohärente Überlagerung der Longitudinalmoden der rekonstruierenden Lichtquelle.

¹⁰ R. J. COLLIER u. K. S. PENNINGTON, *Appl. Phys. Letters* **8**, 14 [1966].

Influence of Time Ordering on Unified Line Profiles

D. VOSSLAMBER

Association EURATOM-CEA, Département de la Physique du Plasma et de la Fusion Contrôlée
Centre d'Etudes Nucléaires, 92260 Fontenay-aux-Roses, France

(*Z. Naturforsch.* **27 a**, 1783—1792 [1972]; received 23 August 1972)

The "width and shift" operator occurring in a previously developed unified theory of Stark broadening by plasma electrons is approximated by different expressions which include time ordering to various orders (up to order four). For the special case of the Lyman- α line in the dipole approximation results also including time ordering to all orders are calculated and compared to the approximate results. Numerical evaluations for this case are presented using the wing expression of the unified theory. A particularly good agreement with the exact profile is obtained for an approximation which maintains time ordering to fourth order. As for the accuracy of un-time-ordered profiles, our results are less optimistic than those of Godfrey et al. The role of an accurate thermal average concerning the effect of time ordering is emphasized.

I. Introduction

In a previous investigation¹, a many-body treatment of spectral line broadening by plasma electrons has been developed using classical path methods. This treatment was combined with the usual quasi-static theory for the plasma ions. Recently, an extension of this work has been presented to include properly the effect of electron correlations². With

respect to the broadening by electron perturbors, the line-shape formulas derived in these treatments are unified in the sense that they are valid from the line center to the far wings, including the transition region between the validity domains of the former impact and quasi-static theories.

The unified formalism essentially divides into two parts: a statistical and a dynamical one. In the statistical part the many-body problem associated to the perturbing electron gas is solved to yield a formal profile expression which apart from the dielectric properties of the plasma only involves binary

Reprint requests to Dr. D. VOSSLAMBER, Association EURATOM-CEA sur la Fusion, Boîte Postale n° 6, F-92260 Fontenay-aux-Roses, France.



Dieses Werk wurde im Jahr 2013 vom Verlag Zeitschrift für Naturforschung in Zusammenarbeit mit der Max-Planck-Gesellschaft zur Förderung der Wissenschaften e.V. digitalisiert und unter folgender Lizenz veröffentlicht: Creative Commons Namensnennung-Keine Bearbeitung 3.0 Deutschland Lizenz.

Zum 01.01.2015 ist eine Anpassung der Lizenzbedingungen (Entfall der Creative Commons Lizenzbedingung „Keine Bearbeitung“) beabsichtigt, um eine Nachnutzung auch im Rahmen zukünftiger wissenschaftlicher Nutzungsformen zu ermöglichen.

This work has been digitalized and published in 2013 by Verlag Zeitschrift für Naturforschung in cooperation with the Max Planck Society for the Advancement of Science under a Creative Commons Attribution-NoDerivs 3.0 Germany License.

On 01.01.2015 it is planned to change the License Conditions (the removal of the Creative Commons License condition "no derivative works"). This is to allow reuse in the area of future scientific usage.

emitter-perturber dynamics. The dynamical part then consists in treating this binary problem explicitly. Both parts are subject to approximations which add to those made from the beginning, namely to the classical path approximation used for all perturbers, to the quasi-static approximation used for the ions³ and to the no-quenching assumption.

We shall first recall briefly the assumptions connected with the statistical part and indicate the corresponding validity conditions. These are found to hold in a wide and realistic domain of plasma and atomic parameters. We then shall turn to the dynamical part of the problem with which our paper will be mainly concerned. Our purpose is to investigate different approximations of the electronic collision operator ("width and shift" operator) with special regard to the effect of time ordering. This will be done by treating the example of the Lyman- α line wing on extending corresponding calculations of Reference¹. (One of the results obtained hereby constitutes a correction of the computer results of Reference¹). We also use a recent result of PFENNIG⁴ who has presented a solution for the time evolution of the emitter under the influence of a classical perturber. Under certain assumptions this solution is exact and thus is expected to provide particularly accurate profiles in the framework of the classical path approximation.

The conclusions we shall draw from our final results will be twofold. They will not only concern the Lyman- α profile itself but also the quality of the approximations used with regard to their possible application to other spectral lines.

II. Validity of the Unified Statistical Treatment

The statistical treatment of the electron broadening as developed in Refs.¹ and ² is based on the following two assumptions:

- (a) Strong emitter-perturber and perturber-perturber collisions must be binary.
- (b) Weak collisions (occurring simultaneously between the emitter and many perturbers) must cause only a small relative change of the emitter state during the correlation time, i. e. mean life-time, of the perturber microfield.

The corresponding validity conditions can be expressed by comparing the strong-collision impact parameter for perturber-emitter collisions, b_{\min} , and the corresponding parameter for perturber-perturber

collisions, b_L , to the mean distance, $\nu^{-1/3}$, between perturbers (ν being the perturber density). We shall restrict ourselves to the case where the emitter is a neutral atom. Then b_{\min} is generally of the order of the Weisskopf radius b_W , but can be smaller in some cases of isolated lines:

$$b_{\min} \lesssim b_W = 3 \hbar n^2 / 2 m_e v_{th},$$

where n is the principal quantum number of the excited state, m_e the electron mass and $v_{th} = (3 k T / m_e)^{1/2}$ the thermal perturber velocity. The Landau length, b_L , is given by

$$b_L = e^2 / m_e v_{th}^2,$$

e being the electron charge.

Assumption (a) is then equivalent to the following inequalities:

$$(a) \quad b_{\min} \ll \nu^{-1/3}, \quad b_L \ll \nu^{-1/3}.$$

Correspondingly, assumption (b) is equivalent to²

$$(b) \quad (b_W / \nu^{-1/3})^{3/2} (b_W / b_L)^{1/2} \ln(b_{\max} / b_{\min}) \ll 1.$$

Here,

$$b_{\max} = \min(\lambda_D, v_{th} / |\omega_{aa'}|),$$

where $\lambda_D = (k T / 4 \pi \nu e^2)^{1/2}$ is the Debye length and $\omega_{aa'}$ some typical frequency characterizing the energy splitting of the excited level group.

For not too high principal quantum number n , condition (b) is contained in the first of conditions (a), so that, in general, the statistical treatment is valid when simultaneous strong collisions are negligibly rare events.

Since the treatment has only been applied to the electron perturbers, for which conditions (a) and (b) are usually well fulfilled (except for large principal quantum number n), we conclude that no serious limitations arise from this statistical part of the formalism.

III. Approximate Treatment of the Collision Operator

The general line shape formulae derived in Refs.¹ and ² under conditions (a) and (b) simplify considerably when applied to those parts of the line wings which lie beyond the plasma frequency. The reasons are that then not only a wing expansion can be used in which the ion and electron contributions superpose additively, but also the dielectric constant in the result of Ref.² can be put equal to

one. We are then led to a wing formula which does not involve collective effects (such as screening or simultaneous perturber actions on the radiating atom) but only binary emitter-perturber dynamics (one-perturber approximation). The wing formula, therefore, is particularly suitable for displaying the effects of approximations used in the dynamical part of the formalism. For this reason, and also in view of our later comparison with wing measurements of the Lyman- α line of hydrogen, we restrict our study to the simplified wing expression, which is given by

$$L(\omega) = \frac{1}{\pi} \sum_{\alpha\beta\alpha'\beta'} \operatorname{Re} \{ \mathbf{D}_{\alpha\beta} \cdot \mathbf{D}_{\alpha'\beta'}^* \cdot \langle \langle \alpha\beta | P_i(\omega) + P_e(\omega) | \alpha'\beta' \rangle \rangle \}. \quad (1)$$

Here, ω denotes the angular frequency measured from some line center ω_0 and \mathbf{D} the atomic dipole moment operator. The summation subscripts α, α' and β, β' label the substates of the upper and lower atomic level groups a and b which are associated to the spectral line under consideration. $\langle \langle \alpha\beta |$ and $| \alpha'\beta' \rangle \rangle$ denote bra and ket vectors of Baranger's doubled atom^{5,6}. P_i and P_e are the ion and electron parts of the profile operator; they are given by

$$P_i(\omega) = (\nu_i e^{3/2}/2) \int_0^\infty F^{-1/2} \delta(\omega + \omega_0 + \hbar^{-1} \bar{H}^0(\mathbf{F})) d^3\mathbf{F}, \quad (2)$$

$$P_e(\omega) = (\omega + \omega_{ba})^{-1} K(\omega) (\omega + \omega_{ba})^{-1}. \quad (3)$$

Here ν_i denotes the ion density; further $\bar{H}^0(\mathbf{F}) \equiv H_b^0(\mathbf{F}) - H_a^{0*}(\mathbf{F})$, $\omega_{ba} = \omega_0 + \bar{H}^0(0)/\hbar$, where $H^0(\mathbf{F})$ is the atomic Hamiltonian under the influence of an electric field \mathbf{F} , subscripts a and b indicating that the corresponding operators act only on states of subspaces a or b, respectively. $K(\omega)$ denotes the electronic collision operator ("width and shift" operator), which may be written in three different forms:

$$K(\omega) = N_e (\omega + \omega_{ba}) \int_0^\infty e^{-i(\omega + \omega_{ba})t} \cdot \langle U(\mathbf{r}, \mathbf{v}, t) - 1 \rangle_{av} dt (\omega + \omega_{ba}), \quad (4a)$$

$$= -\frac{N_e}{\hbar} \int_0^\infty \langle \bar{V}(\mathbf{r} + \mathbf{v}t) e^{-i(\omega + \omega_{ba})t} \cdot U(\mathbf{r}, \mathbf{v}, t) \rangle_{av} dt (\omega + \omega_{ba}), \quad (4b)$$

$$= \frac{N_e}{\hbar^2} \int \langle \bar{V}(\mathbf{r} + \mathbf{v}t) e^{-i(\omega + \omega_{ba})t} \cdot U(\mathbf{r}, \mathbf{v}, t) \bar{V}(\mathbf{r}) \rangle_{av} dt. \quad (4c)$$

In these expressions, N_e denotes the total number of electrons. $U(\mathbf{r}, \mathbf{v}, t)$ is the time evolution operator (in the interaction representation) of the "doubled atom"^{5,6} interacting with one perturbing charge moving on the straight line $\mathbf{r} + \mathbf{v}t$. It is defined by the Schrödinger equation¹

$$\partial U / \partial t = - (i/\hbar) \tilde{V}(\mathbf{r}, \mathbf{v}, t) U, \quad U(\mathbf{r}, \mathbf{v}, 0) = 1 \quad (5)$$

where

$$\tilde{V}(\mathbf{r}, \mathbf{v}, t) = e^{i\bar{H}^0(0)t/\hbar} \bar{V}(\mathbf{r} + \mathbf{v}t) e^{-i\bar{H}^0(0)t/\hbar}, \quad \bar{V} = V_b - V_a^*. \quad (5a)$$

V being the interaction part of the total Hamiltonian $H^0(0) + V(\mathbf{r} + \mathbf{v}t)$. Further, the symbol $\langle \rangle_{av}$ denotes a thermal average in the six-dimensional phase space taken with the Maxwellian velocity distribution:

$$\langle G(\mathbf{r}, \mathbf{v}) \rangle_{av} \equiv \frac{\nu_e}{N_e} \left(\frac{m_e}{2\pi k T_e} \right)^{3/2} \cdot \int d^3r \int d^3v \exp\{-m_e v^2/2kT_e\} G(\mathbf{r}, \mathbf{v})$$

where G is any operator depending on position \mathbf{r} and velocity \mathbf{v} .

The three different forms (4a–c) of the collision operator can be obtained from one another by essentially using Eq. (5) in connection with integrations by parts over t in the Equations (4). The form (4b)⁷ can be derived from (4a) by replacing U with the expression which is obtained from Eq. (5) by integrating it formally over time (from zero to t). Note that $\langle V(\mathbf{r} + \mathbf{v}t) \rangle_{av} = 0$ because the plasma is assumed to be homogeneous and the radiating atom is neutral. The derivation of the form (4c)⁸ from (4b) is somewhat more involved and is described in detail in the Appendix.

We stated that the three forms (4a–c) of the collision operator are identical. This, of course, is only true if in each of these forms the time evolution operator U is taken to be the exact solution of Equation (5). If an approximate solution is used, then the three expressions (4a–c) spread out, and the deviations between the corresponding profiles can generally be considered as a measure for the uncertainty connected with the approximations used. Note that no spread occurs when the exact solution of an approximated Eq. (5) is employed, provided that in Eqs. (4) the same approximations for $\bar{H}^0(0)$ and \bar{V} are used as in Equation (5).

In most cases the exact solution of Eq. (5) cannot be written, even if $H^0(0)$ and \bar{V} are approximated. An exception is the case where $\bar{H}^0(0)$ is com-

pletely degenerate (hydrogen), and where \bar{V} is replaced by its dipole approximation⁴. This case will be treated in detail in Section IV.

In the general case Eq. (5) must be solved approximately. It is not sufficient, however, to write the solution as a perturbation expansion to finite order, because then the unified character of the collision operator $K(\omega)$ would be lost. In fact, as one increases ω on the line profile, more and more orders in the perturbation \bar{V} would be required, and eventually all orders would be necessary as one moves into the quasi-static region. It is well-known that second order perturbation theory, for instance, only describes the impact region, where weak collisions are dominant, and that even there a strong collision cut-off is needed to avoid divergencies at small impact parameters.

A more suitable type of approximation consists in first writing the time evolution operator as an exponential^{1, 9}

$$U(\mathbf{r}, \mathbf{v}, t) = \exp \{ -i W(\mathbf{r}, \mathbf{v}, t) \} \quad (6)$$

and then looking for convenient approximations for the new operator W . The exponential form is suggested by the formal and exact expression

$$U(\mathbf{r}, \mathbf{v}, t) = Z \exp \left\{ - (i/\hbar) \int_0^t \tilde{V} d\tau \right\} \quad (7)$$

where Z is the time ordering operator¹⁰.

In our treatment we employ an algorithm for successive approximate solutions $U^{(k)} = \exp \{ -i W^{(k)} \}$ which has been derived in Ref. ⁹ for equations of the type (5) [with $\tilde{V}(t)$ being a more arbitrary time-dependent operator]. These approximate solutions conserve several important properties of the exact evolution operator U , such as its unitarity and the boundedness of W/μ , where μ is a typical coupling parameter characterizing the strength of $\tilde{V}(t)$. Further, the approximations $U^{(k)}$ are identical with the exact solution ($W^{(k)} = 0$ for $k \geq 2$) if $\tilde{V}(t)$ commutes with its integral over t . Finally, when developed in powers of \tilde{V} , the expressions $U^{(k)}$ agree with the perturbation expansion of U up to order k , i. e. they maintain time ordering up to order k .

Let us consider the consequences of these properties for corresponding approximate solutions of Eq. (5) with regard to their application in Equations (4a–c). The $(\mathbf{r}, \mathbf{v}, t)$ -space over which the integrations in these equations occur, may be thought to be split up into several characteristic domains.

A first domain (I) is that in which the absolute values of typical matrix elements of $\hbar^{-1} \int_0^t \tilde{V} d\tau$ or $W^{(k)}$ are small compared with unity (they are allowed to reach the order of unity for high enough k), a second one (II) is that in which these values are large compared with unity. We are then left with a third domain (III) in which the values are of the order of unity. The domain I corresponds to weak collisions ($|\mathbf{r} \times \mathbf{v}|/|\mathbf{v}| \gg b_W$) or to the first stage (small times t) of medium or strong collisions. In this domain the approximations $U^{(k)}$ are at least as accurate as perturbation results to order k , but have the advantage to be unitary and thus not to falsify the normalisation of the atomic wavefunctions. The domain II corresponds to strong collisions ($|\mathbf{r} \times \mathbf{v}|/|\mathbf{v}| \ll b_W$) for not too small times t . In this domain the expressions $U^{(k)}$ [just as the exact solution (7)] constitute rapidly oscillating factors in the integrand of Eqs. (4a–c) and thus provide negligible contributions to the total integral. The domain III can again be divided into two parts, a region III a where the initial perturber positions are very close to the radiating atom (say $|\mathbf{r}| \ll b_W$) and a region III b corresponding to medium or distant initial perturber positions. In case III a the collision is strong, but the time is very short, and $\hbar^{-1} \int_0^t \tilde{V}(\tau) d\tau$ becomes of order unity before $\tilde{V}(t)$ has changed appreciably. Indeed, during a time $t \approx (|\mathbf{r}|/b_W) (|\mathbf{r}|/|\mathbf{v}|)$, the potential \tilde{V} remains practically constant (its characteristic variation time being $|\mathbf{r}|/|\mathbf{v}|$ ¹¹), while typical matrix elements of $\hbar^{-1} \int_0^t \tilde{V}(\tau) d\tau \approx \tilde{V}(0) t/\hbar$ are on the order of one [assuming $\tilde{V}(0)$ of the order of $(a_0 n^2)(e^2/r^2)$, a_0 being the Bohr radius]. In region III a, therefore, the potential \tilde{V} can be considered as time-independent and then trivially commutes with its time integral. Consequently, the expressions $U^{(k)}$ all become exact (to the extent as \tilde{V} is constant) and are equal to the “quasi-static” time evolution operator $\exp \{ -i t \tilde{V}(0)/\hbar \}$.

From these considerations we may argue that the approximations $U^{(k)}$ are satisfactory in regions I, II, and III a, but that they are not sufficient in region III b¹². Therefore, this region has to be kept small [regarding its contribution to the total integrals in Eqs. (4a–c)] by choosing k sufficiently high. Indeed, for increasing k , region III is taken

up more and more by region I, because then we may admit that in region I the operator $\hbar^{-1} \int \tilde{V} d\tau$ has matrix elements comparable to unity instead of requiring that they be much smaller than unity.

It is worthwhile to study the influence of the various regions of the $(\mathbf{r}, \mathbf{v}, t)$ -space on the different frequency domains of the line profile. For small frequency separation from the line center ($\omega < \omega_p$) weak completed collisions are dominant, i. e. here the influence of region I prevails. For the small fraction of strong collisions the arguments of region II hold, whereas a slight uncertainty arises from collisions of medium strength (region III b) if k is not chosen sufficiently high. The difficulties of the usual perturbation treatment, however, leading to divergent integrals in Eqs. (4 a–c) and necessitating strong-collision cut-offs, do not occur in this formalism. When ω increases beyond the plasma frequency (but stays below the Weisskopf frequency $\omega_W = v_{th}/b_W$) the relative importance of weak collisions diminishes. However, because of the shorter times $t \approx \omega^{-1}$ under consideration, region I now includes part of the strong collisions. The other part belongs to regions II and III b; the latter region again introduces an uncertainty and can only be reduced by choosing k sufficiently high. For frequency separations ω much larger than the Weisskopf frequency ω_W (quasi-static wing) all initial perturber positions are very close to the radiating atom. Corresponding collisions start in region I, pass through III a and eventually arrive in region II. They never involve region III b. This is why the approximations $U^{(k)}$ yield the exact quasi-static limit on the far line wings.

We may summarize our considerations by stating that the approximations $U^{(k)}$ reproduce the correct limits of the line profile in the impact regime (because of the predominance of weak collisions) as well as for the quasi-static wings. In the intermediate region the quality of the approximations depends on the order k chosen in the algorithm for the $U^{(k)}$.

Of course, it cannot be deduced from these qualitative arguments which value of k must be chosen in order to attain a given degree of accuracy in the final results. This seems to be possible only in an empirical way, e. g. by studying the spread in the different approximate results or (in special cases) by comparing approximate results with an exact result. This method will be discussed in detail in the next section.

Practical calculations will generally have to be restricted to $k=1$ and $k=2$. For these values the algorithm developed in Ref. ⁹ yields the following two approximate solutions of Equation (5):

$$U^{(1)} = \exp\{-iW^{(1)}\} = \exp\left\{-\frac{i}{\hbar} \int_0^t \tilde{V}(\tau) d\tau\right\}, \quad (8)$$

$$U^{(2)} = \exp\{-iW^{(2)}\}$$

with

$$W^{(2)} = \hbar^{-1} \int_0^t \exp\{iW^{(1)}/2\} \tilde{V} \exp\{-iW^{(1)}/2\} d\tau. \quad (9)$$

Inserting these approximations into the three forms (4 a–c) of the collision operator yields six expressions for the line profile. Let us denote the corresponding approximations for the collision operator by $K_m^{(k)}$ ($k=1, 2$; $m=0, 1, 2$), m denoting the number of \tilde{V} -factors accompanying the time evolution operator U in the form chosen for K , and k indicating that the approximation $U^{(k)}$ is used in K . With these definitions we have $m=0$ in Eq. (4 a), $m=1$ in Eq. (4 b), and $m=2$ in Equation (4 c). One of the six expressions, namely $K_2^{(2)}$, is particularly interesting regarding the behaviour of its integrand in region I of the $(\mathbf{r}, \mathbf{v}, t)$ -space. Indeed, since the integrand has two \tilde{V} -factors accompanying the approximate time evolution operator $U^{(2)}$, which is correct to second order, time ordering is maintained to fourth order in this expression. The corresponding result is therefore expected to be more accurate than the other five expressions for the collision operator, which are correct to lower order only. Note that before the thermal average is carried out in Eqs. (4 a–c), the order to which the integrands include time ordering is $k+m$. After the averaging, odd orders vanish and even $K_0^{(1)}$ becomes correct to second order because the incorrect second order terms of its integrand cancel after the integration; therefore, all the integrated $K_m^{(k)}$ except $K_2^{(2)}$ are correct to second order.

IV. Application to the Lyman- α Wing

For a numerical evaluation in the case of the Lyman- α line of hydrogen, we use the dipole approximation in the interaction potential, i. e. we write

$$V(\mathbf{r}) = -e\mathbf{D} \cdot \mathbf{r}/|\mathbf{r}|^3. \quad (10)$$

This not only simplifies the mathematics but also enables us to use PFENNIG's expression for the time evolution operator⁴ (which we call U^P) in addition to our approximations $U^{(1)}$ and $U^{(2)}$. Indeed, after introducing the approximation (10) into Eq. (5), where $\bar{H}^0(0)$ is now assumed to be degenerate, U^P constitutes the exact solution and correspondingly leads to a collision operator (denoted by K^P) which is exact in the framework of the dipole and degeneracy assumptions¹³. Under these assumptions, we thus are able to check the quality of our approximations by comparing the corresponding approximate profiles (based on the collision operators $K_m^{(k)}$) with the exact profile based on K^P .

The evaluation of one of the six forms $K_m^{(k)}$, namely $K_1^{(2)}$, has already been described in detail in Reference¹. The other five forms, as well as K^P , can be treated in a very similar fashion. In order to evaluate the forms $K_m^{(1)}$, an explicit expression for $U^{(1)}$ is needed. This can be obtained from $U^{(2)}$, i. e. from Eqs. (35) and (32) of Ref. ¹ by putting $y=0$ in Equation (32). Further, for the evaluation of K^P , the operator U^P is needed in spherical coordinates. If we use Eq. (4 c), only the first matrix element U_{11}^P enters the final wing formula; this element is

$$U_{11}^P(x, \vartheta) = \frac{1}{1+x^2} (1+x^2 \cos \sqrt{1+x^2} \vartheta) \quad (11)$$

where the angle ϑ is defined as in Reference¹ and $x=3\lambda/b$, $\lambda=\hbar/m_e v$ being the De Broglie wave length of the perturbing electron and b its impact parameter.

Since the detailed calculations follow very closely the lines indicated in Ref. ¹, we may here restrict ourselves to present the different results for the function

$$F(\Omega) = L_e(\omega)/L_i(\omega),$$

where L_e and L_i are defined in an obvious way from Eq. (1), and $\Omega = (\hbar/2kT)\omega$. The function $F(\Omega)$ represents the electron contribution to the line wing, divided by the Holtsmark asymptote (which is the same for electrons and ions) and therefore tends to 1 as $\Omega \rightarrow \infty$.

Let us denote by $F_m^{(k)}$ and F^P the approximations of F calculated on using $K_m^{(k)}$ and K^P , respectively. Using further the notations

$$A(x, \vartheta) = \int_0^\vartheta \left[\cos \psi' \cos^2 \left(\frac{x}{2} \sin \frac{\psi}{2} \right) + \sin^2 \left(\frac{x}{2} \sin \frac{\psi}{2} \right) \right] d\psi,$$

$$B(x, \vartheta) = \sin^2 \frac{\vartheta}{2} + \frac{2}{x} \sin \frac{\vartheta}{2} \sin \left(x \sin \frac{\vartheta}{2} \right) - \frac{4}{x^2} \sin^2 \left(\frac{x}{2} \sin \frac{\vartheta}{2} \right),$$

$$C(x, \vartheta) = \int_0^\vartheta \sin \frac{\psi}{2} \sin \left(x \sin \frac{\psi}{2} \right) d\psi,$$

$$Y(\Omega, x, \vartheta, \Theta) = 2[3\Omega \sin \vartheta/x \sin \Theta \sin(\Theta - \vartheta)]^{1/2}, \\ A = (A^2 + B^2 + C^2)^{1/2},$$

we have the following results for the different $F_m^{(k)}$:

$$F_m^{(k)}(\Omega) = 4\sqrt{3}/\pi^{3/2} \int_0^\infty dx \int_0^\pi d\vartheta g_m^{(k)}(x, \vartheta) \cdot \int_\vartheta^\pi d\Theta h_m(\Omega, x, \vartheta, \Theta), \quad (12)$$

where

$$\begin{aligned} h_0 &= [\Omega^{1/2} Y^3 \text{kei}' Y]/2 x^3 \sin^2 \vartheta, \\ h_1 &= -[6 \Omega^{3/2} \text{kei} Y]/[x^3 \sin^2(\Theta - \vartheta)], \\ h_2 &= -[\Omega^{1/2} Y \text{ker}' Y \cos \vartheta]/x, \\ g_0^{(1)} &= \sin^2[x \sin(\vartheta/2)], \\ g_0^{(2)} &= (1 + C^2/A^2) \sin^2(xA/2), \\ g_1^{(1)} &= \cos \frac{\vartheta}{2} \sin \left(2x \sin \frac{\vartheta}{2} \right), \\ g_1^{(2)} &= (A/A) \sin(xA) + (2BC/A^2) \sin^2(xA/2), \\ g_2^{(1)} &= \cos[2x \sin(\vartheta/2)], \\ g_2^{(2)} &= \cos(xA) + (2C^2/A^2) \sin^2(xA/2). \end{aligned}$$

Here, kei and ker denote Kelvin functions, kei' and ker' being their derivatives.

For F^P , three equivalent formulations corresponding to Eqs. (4 a-c) are available, each of them being obtained from the others by an integration by parts over ϑ . We here only indicate the form corresponding to Equation (4 c)¹⁴,

$$F^P(\Omega) = \frac{4\sqrt{3}}{\pi^{3/2}} \int_0^\infty dx \int_0^\pi d\vartheta U_{11}^P(x, \vartheta) \cdot \int_\vartheta^\pi d\Theta h_2(\Omega, x, \vartheta, \Theta), \quad (13)$$

where U_{11}^P is given by Equation (11).

In Equations (12) and (13) the integration over $x=3\lambda/b$ is extended to infinity though for $b \lesssim \lambda$ the semi-classical approximation breaks down. Such a procedure has been justified in Ref. ¹ with interruption theory arguments and with the fact that for large frequency separations from the line center ($\omega \gtrsim \omega_W$) even wave packets with size below λ do not spread out considerably during the very short

times ω^{-1} of interest. These arguments, of course, are qualitative and require a more detailed study, preferably by using purely quantum-mechanical theories^{15, 16}. In order to investigate the contribution of the impact parameter domain $b < \lambda$ in the semi-classical treatment, also functions $F_c^P(\Omega)$ and $F_{oc}^{(1)}(\Omega)$ have been calculated (the latter for a comparison with Ref. 17) corresponding to $F^P(\Omega)$ and $F_0^{(1)}(\Omega)$ with a lower impact parameter cut-off at $b = \lambda$, i. e. to an upper limit of the x -integration at $x = 3$ in Eqs. (12) and (13)¹⁸.

The different approximations $F_m^{(k)}$, F^P , $F_{oc}^{(1)}$, F_c^P for the function $F(\Omega)$ have been evaluated numerically¹⁹. The corresponding results $I_m^{(k)}$, I^P , $I_{oc}^{(1)}$, I_c^P for the total relative intensity

$$I(\Delta\lambda) = 1 + F(hc\Delta\lambda/2\lambda^2 kT)$$

(representing the sum of the ion and electron contributions to the line wing) are plotted in Figs. 1 and 2 as functions of the wave length separation $\Delta\lambda = (2\lambda^2 kT/hc)\Omega$. It should be noted with regard to the true profile that the left ends of the curves are slightly uncertain, because for them Debye screening and higher terms of the wing expansion may have some importance. Furthermore, the right sides of the dashed curves ($I_{oc}^{(1)}$, I_c^P) fall off too steeply for reasons given in¹⁸. In Fig. 1, the

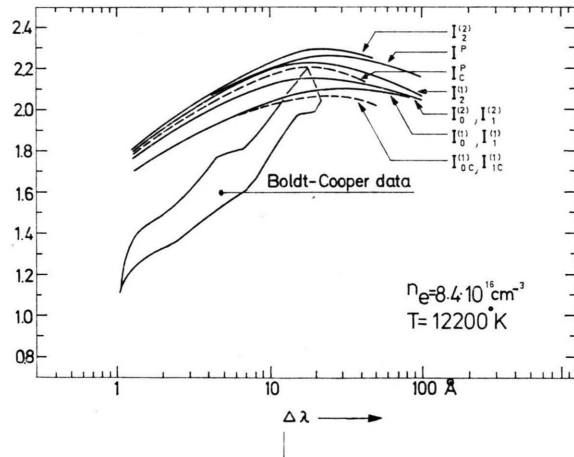


Fig. 1. Different theoretical wing profiles of the Lyman- α line of hydrogen in comparison to measurements of Boldt and Cooper. The intensities are represented relative to the ionic Holtsmark asymptote.

theoretical results are compared to the experimental data of BOLDT and COOPER²⁰ (which have been essentially reproduced by a recent experiment of

FUSSMANN^{20a}), in Fig. 2 the same comparison is made with the experiment of ELTON and GRIEM²¹. The agreement is better in the latter case; however, it has to be noted that in this experiment the intensity measurements were relative and the absolute

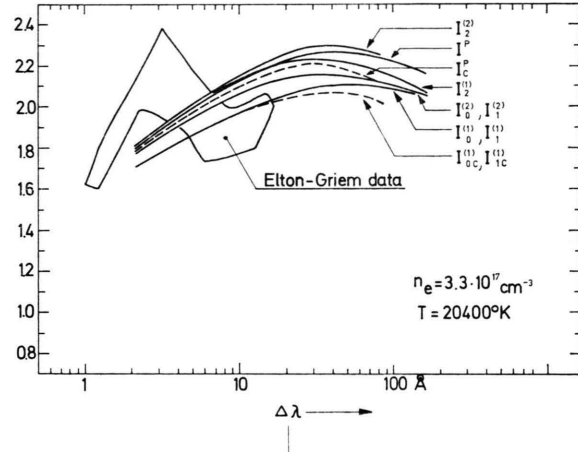


Fig. 2. Different theoretical wing profiles of the Lyman- α line of hydrogen in comparison to measurements of Elton and Griem. The intensities are represented relative to the ionic Holtsmark asymptote.

determination has been made using theoretical arguments. Since also the slope of the profile found in Refs. 20 and 20a does not agree with that of Ref. 21, no conclusion can be drawn from this comparison concerning the quality of our theoretical results. From this point of view it is more interesting to compare the theoretical profiles among themselves.

The influence of time ordering in the evolution operator can be seen by comparing the approximate profiles $I_m^{(k)}$ with the curve I^P , which is calculated with PFENNIG's⁴ evolution operator and is therefore exact under the assumptions made in this section. As expected, a particularly good agreement is obtained for the profile $I_2^{(2)}$, in which time ordering is maintained to fourth order. This shows that it might be sufficient in general to choose $k=2$ in the algorithm for $U^{(k)}$, provided a form containing two \bar{V} -factors is used for the collision operator²². The general tendency of the profiles is to approach I^P as $k+m$ increases²³.

This indicates that also odd orders in the potential \bar{V} may be important even though they vanish after a term by term integration of the series expansion in powers of \bar{V} of the integrand in Equations (4a-c). The reason seems to be that if the integrand is correct to higher orders, it also remains

valid closer to the region of strong collisions, where a series expansion cannot be made and where arguments cannot be based on such an expansion. No profound explanation seems to exist for the nearly perfect coincidence between the curves $I_0^{(1)}$ and $I_1^{(1)}$ on the one hand, and between $I_0^{(2)}$ and $I_1^{(2)}$ on the other hand²⁴. In the impact limit (for small $\Delta\lambda$) nearly all profiles approach the exact result. Exceptions are the curves $I_0^{(1)}$, $I_1^{(1)}$ and $I_{oc}^{(1)}$ whose agreement with the exact profile is rather poor over the entire line profile.

One of these latter approximations ($I_{oc}^{(1)}$) corresponds closely to one discussed by GODFREY et al.¹⁷. It was compared by these authors to a time-ordered result obtained by integrating the Schrödinger Equation (5) numerically. Their time-ordered and un-time-ordered results should correspond to our profiles I_c^P and $I_{oc}^{(1)}$, except for the following differences: (a) In Ref. ¹⁷ a Debye cut-off is used (the profile being calculated also in the line center), while no screening effects are contained in our wing formula; (b) in Ref. ¹⁷ a strong collision cut-off at the De Broglie wavelength λ is applied to the atom-perturber distance, while in our treatment a corresponding cut-off at λ is used for the impact parameter; (c) in Ref. ¹⁷ the comparison between the time-ordered and un-time-ordered results is made by using a representative thermal velocity, while in our treatment the thermal average is carried out correctly.

A comparison between the numerical results of both treatments shows that the effect of time ordering is larger in our results than in those of Ref. ¹⁷ in a wide region of the line profile. The effects are comparable in the impact region, where the relevant parts of the collision operator change by about 11% in both cases. (From this we may conclude that we would find comparable effects also in the central part of the line if we did a complete profile calculation, too.) As we go towards higher frequency separations ($\omega > \omega_p$), however, we find larger relative deviations between the time-ordered and un-time-ordered profiles than those indicated in Reference ¹⁷. Even in the case of zero ion field, which yields the highest effect of time ordering in Ref. ¹⁷, we find deviations up to 12.5% in the region between the plasma frequency and the Weisskopf frequency, while corresponding deviations in Ref. ¹⁷ do not exceed 9%. Furthermore, in our results the deviations extend to larger frequency separations than in Re-

ference ¹⁷. For the case calculated there ($T = 20\,000$ °K), we find still a deviation of about 9% at $\Delta\lambda = 90$ Å, while in Ref. ¹⁷ the deviation has dropped off to zero at this wavelength.

The question arises whether this disagreement may be due to some of the differences (a–c) mentioned above. The difference (a) is very unlikely to cause any discrepancy on the far wings. If screening would play a role at all, it would rather enhance the relative effect of time ordering in our treatment because distant collisions are known to be unaffected by time ordering. As for difference (b), which might have some importance for large frequency separations ($\omega \gtrsim \omega_W$), the allowance for collisions with impact parameters below λ in our treatment (in connection with a distance cut-off at λ) is also expected to increase the effect of time ordering rather than to decrease it. Thus, apart from numerical uncertainties²⁵, the only plausible cause for the observed disagreement seems to be difference (c). In fact, the use of one representative thermal velocity does not take account of the fact that for a given initial perturber distance and impact parameter (especially when the latter is not far from the Weisskopf radius) slow collisions ($v < v_{th}$) are stronger and involve higher effects of time ordering than fast collisions ($v > v_{th}$). Therefore, regarding the importance of time ordering, there is some shift from the thermal velocity towards smaller velocities. As compared to the case where just one velocity equal to the thermal one is used, a full thermal average thus leads to a larger total broadening and to higher effects of time ordering.

It is this same reason which probably also explains the significant discrepancy between our profile I^P and a recently published result²⁶ which is based on the evolution operator U^P and calculated by using just a thermal velocity instead of carrying out the full thermal average. It is also interesting to compare our results with profiles obtained by employing the adiabatic approximation for the evolution operator²⁷. The difference between these results and ours may only be partially due to the use of the adiabatic approximation and might probably be reduced by introducing the full thermal average into the treatment of Reference ²⁷.

Finally, as far as early calculations for the Lyman- α profile are concerned, we find a remarkable agreement between our curve I^P and the result of

Ref. ²⁸ up to $\Delta\lambda \approx 10 \text{ \AA}$ (in the case of Fig. 1) and between our curves $I_0^{(2)}$, $I_1^{(2)}$ and the result of Ref. ²⁹ from $\Delta\lambda = 3 \text{ \AA}$ to $\Delta\lambda = 30 \text{ \AA}$.

V. Concluding Remarks

We have investigated different possibilities of approximating the collision operator in a previously developed unified theory for Stark Broadening by plasma electrons. The first two members of an algorithm for exponential approximations of the time evolution operator have been used in different forms of the collision operator to yield profiles in which time ordering is maintained to various orders, up to order four. Numerical calculations have been done for the special case of the Lyman- α line wing using the dipole approximation for the perturber-atom interaction potential. For this case also the profile based on the "exact" time evolution operator has been calculated and compared to the various approximations. A particularly good agreement is found between the exact result and that approximation which maintains time ordering to fourth order. From this we may conjecture that also in more general cases where the exact result is not available, it might be a good approximation to combine an exponential "second-order" time evolution operator $U^{(2)}$ with a form for the collision operator which contains two potential factors \bar{V} [Equation (4c)].

As far as the difference between the exact and completely un-time-ordered profiles is concerned, we have found larger deviations than GODFREY et al. ¹⁷. This difference appears to be due, at least partially, to the way in which the thermal average is calculated. One of our conclusions is that with respect to the total amount of broadening and to the effect of time ordering, the use of just one thermal velocity might not be sufficient.

Appendix

Defining the operator

$$Q(\mathbf{r}, \mathbf{v}, t) \equiv \exp \left\{ - (i/\hbar) \bar{H}^0 t \right\} U(\mathbf{r}, \mathbf{v}, t)$$

which satisfies Eq. (13) of Ref. ¹ and obeys the relation

$$Q(\mathbf{r} - \mathbf{v}t, \mathbf{v}, t) = Q^{-1}(\mathbf{r}, \mathbf{v}, -t),$$

and using

$$dQ^{-1}/dt = -Q^{-1}(dQ/dt)Q^{-1},$$

we get the following equation for $Q(\mathbf{r} - \mathbf{v}t, \mathbf{v}, t)$:

$$\frac{d}{dt} Q(\mathbf{r} - \mathbf{v}t, \mathbf{v}, t) = -\frac{i}{\hbar} Q(\mathbf{r} - \mathbf{v}t, \mathbf{v}, t) \cdot [\bar{H}^0 + \bar{V}(\mathbf{r} - \mathbf{v}t)].$$

In the interaction representation this equation reads

$$\frac{d}{dt} R(\mathbf{r} - \mathbf{v}t, \mathbf{v}, t) = -\frac{i}{\hbar} R(\mathbf{r} - \mathbf{v}t, \mathbf{v}, t) \cdot \exp \left\{ - (i/\hbar) \bar{H}^0 t \right\} \bar{V}(\mathbf{r} - \mathbf{v}t) \exp \left\{ - (i/\hbar) \bar{H}^0 t \right\}, \quad (\text{A.1})$$

where

$$R \equiv Q \exp \left\{ (i/\hbar) \bar{H}^0 t \right\} = \exp \left\{ - (i/\hbar) \bar{H}^0 t \right\} U \exp \left\{ (i/\hbar) \bar{H}^0 t \right\}.$$

Integrating Eq. (A.1) formally over time and re-expressing R in terms of U yields

$$U(\mathbf{r} - \mathbf{v}t, \mathbf{v}, t) = 1 - \frac{i}{\hbar} \int_0^t \exp \left\{ (i/\hbar) \bar{H}^0 (t - \tau) \right\} \cdot U(\mathbf{r} - \mathbf{v}\tau, \mathbf{v}, \tau) \bar{V}(\mathbf{r} - \mathbf{v}\tau) \cdot \exp \left\{ - (i/\hbar) \bar{H}^0 (t - \tau) \right\} d\tau. \quad (\text{A.2})$$

Because of the homogeneity of the plasma, the average quantity occurring in Eq. (4b) can be written as

$$\langle \bar{V}(\mathbf{r} + \mathbf{v}t) \exp \left\{ -i(\omega + \omega_{ba})t \right\} U(\mathbf{r}, \mathbf{v}, t) \rangle_{\text{av}} = \langle \bar{V}(\mathbf{r}) \exp \left\{ -i(\omega + \omega_{ba})t \right\} U(\mathbf{r} - \mathbf{v}t, \mathbf{v}, t) \rangle_{\text{av}},$$

and $U(\mathbf{r} - \mathbf{v}t, \mathbf{v}, t)$ can be replaced by the expression (A.2). By an integration by parts over time and using again the homogeneity of the plasma, one then readily arrives at Equation (4c).

¹ D. VOSLAMBER, Z. Naturforsch. **24a**, 1458 [1969]; Erratum **26a**, 1558 [1971].

² H. CAPES and D. VOSLAMBER, Phys. Rev. A **5**, 2528 [1972].

³ More rigorously, the separation is not between ions and electrons, but between the low frequency component and the high frequency component of the plasma microfield. For more details see Ref. ², where also references to the corresponding literature are given.

⁴ H. PFENNIG, Phys. Letters **34 A**, 292 [1971]; Z. Naturforsch. **26a**, 1071 [1971]; J. Quant. Spectr. Rad. Transfer **12**, 821 [1972].

⁵ M. BARRANGER, in: Atomic and Molecular Processes (ed. D. R. BATES), Academic Press, New York 1962.

⁶ H. R. GRIEM, Plasma Spectroscopy, McGraw-Hill, New York 1964.

⁷ Only this form has been presented in Ref. ¹.

⁸ This form corresponds to that given in Ref. ² for $\varepsilon(p, k)=1$.

⁹ D. VOSLAMBER, J. Math. Anal. Applic. **37**, 403 [1972].

¹⁰ S. SCHWEBER, An Introduction to Relativistic Quantum Field Theory, Harper & Row Publishers, New York 1962, pp. 330-334.

¹¹ The variation due to the exponential factors in Eq. (5a) is slower if the largest energy separation in the upper level group, corresponding to an allowed transition, is smaller than $\hbar |v|/b_W$.

- ¹² Note, however, that no singular behaviour can arise in this region because the approximations $U^{(k)}$ are unitary and therefore bounded, just as the exact expression (7).
- ¹³ When the calculation is not restricted to the line wing, Eq. (5) involves $\bar{H}^0(F)$ instead of $H^0(0)$. However, in order that U^P be the exact solution, the dependence on F has to be suppressed.
- ¹⁴ The other two forms have also been calculated and used as numerical tests for the first one.
- ¹⁵ D. VOSLAMBER, *Physics Letters* **40 A**, 266 [1972].
- ¹⁶ N. TRAN MINH and H. VAN REGEMORTER, *J. Phys. B* **5**, 903 [1972].
- ¹⁷ J. T. GODFREY, C. R. VIDAL, E. W. SMITH, and J. COOPER, *Phys. Rev. A* **3**, 1543 [1971]. — *Natl. Bur. Stand. (U.S.) Monograph No. 121*.
- ¹⁸ It should be noted that when ω is not much smaller than kT/\hbar , a cut-off at $\tilde{\lambda}$ is not a realistic limitation of the region where the classical path approximation is valid. As pointed out in Ref. ¹, for large ω the wave packet diffusion is required to stay small only during times ω^{-1} which may be smaller than the relevant collision times b/v . Correspondingly, the impact parameter b_c delimiting the classical domain is then $(\hbar/m\omega)^{1/2}$ instead of $\tilde{\lambda}$. Both become equal for $\omega = kT/\hbar$ (here the theory breaks down because it is based on a factorisation of the total density operator); however, b_c should be taken smaller than $\tilde{\lambda}$ already for $\omega \gtrsim \omega_W$ in order to have smooth transition between the two limiting expressions $\tilde{\lambda}$ and $(\hbar/m\omega)^{1/2}$.
- ¹⁹ Direct integration methods have been used without employing the Monte Carlo method used in Ref. ¹.
- ²⁰ G. BOLDT and W. S. COOPER, *Z. Naturforsch.* **19 a**, 968 [1964].
- ^{20a} G. FUSSMANN, *Phys. Letters* **41 A**, 155 [1972].
- ²¹ R. C. ELTON and H. R. GRIEM, *Phys. Rev.* **135 A**, 1550 [1964].
- ²² This result also clearly refutes the statement in Ref. ¹⁶ that all exponential forms of the S -matrix which do not take proper account of the time ordering operator are unable to give any information on strong collisions.
- ²³ Note that $I_1^{(2)}$ represents the corrected numerical result of Ref. ¹.
- ²⁴ Small deviations were found within the numerical error limits.
- ²⁵ Note that the numerical integration of the Schrödinger equation in Ref. ¹⁷ is done only for impact parameters of the interval $0.3 \tilde{\lambda} < b < 10 \tilde{\lambda}$. — Outside this interval approximations are used. Also the Fourier transform in the collision operator is calculated with approximative methods.
- ²⁶ V. S. LISITSA and G. V. SHOLIN, *J. Quant. Spectrosc. Radiat. Transfer* **12**, 985 [1972].
- ²⁷ V. I. KOGAN and V. S. LISITSA, *J. Quant. Spectrosc. Radiat. Transfer* **12**, 881 [1972].
- ²⁸ H. R. GRIEM, *Astrophys. J.* **136**, 422 [1962].
- ²⁹ H. R. GRIEM, *Phys. Rev.* **140 A**, 1140 [1965].

Theory of Damped Polaritons

L. MERTEN * and G. BORSTEL *

Department of Physics, University of Southern California, Los Angeles, California 90007

(*Z. Naturforsch.* **27 a**, 1792—1797 [1972]; received 5 June 1972)

The basic equations of damped polaritons in orthorhombic crystals and those of higher symmetry are set up. From these basic equations a general dispersion equation for the complex frequencies (real frequency and damping factor) is derived.

Essential differences of the dispersion curves are demonstrated for the case of purely temporally damped polaritons (ω complex, k real) and of purely spatially damped polaritons (ω real, k complex). A detailed discussion and numerical evaluations are given for ZnF_2 as an example.

1. Introduction

In the past the properties of polaritons in general have been treated in the harmonic approximation, i. e., the effect of damping has been neglected in theory. Nevertheless, the damping of polaritons is an important physical quantity which determines e. g., the natural line width of Raman lines, the losses in stimulated Raman effect or the detailed shape of the IR-spectra. A more exact investigation of damping of polaritons has also become of immediate interest because of a controversy which arose among

several authors resulting from evident discrepancies between the hitherto existing theory and the experimental results ¹⁻³. Essentially these discrepancies lay in the existence of a limiting momentum k_c in the $\omega(k)$ diagram as well as a turnaround of the polariton branch at this k_c demanded by theory. In contrast to the experimental results, these conclusions from theory include the nonexistence of long optical phonons in the Raman effect as well as an additional polariton branch which never has been detected experimentally.

Reprint requests to Lehrstuhl Prof. Dr. L. MERTEN, Fachbereich Physik der Universität Münster, D-4400 Münster, Schloßplatz 7.

* Permanent address: Fachbereich Physik der Universität Münster, Physikalisches Institut.